# Model-Based Conifer-Crown Surface Reconstruction from High-Resolution Aerial Images

Yongwei Sheng, P. Gong, and G.S. Biging

## Abstract

*Knowledge of tree-crown parameters such as height, shape, and crown closure is desirable in forest and ecological studies, but those parameters are difficult to measure on the ground. The stereoscopic capability of high-resolution aerial images provides a method for crown-surface reconstruction. However, existing digital photogrammetry packages, designed to map terrain surfaces, cannot accurately extract tree-crown surfaces, particularly for conifer-crowns with steep vertical profiles.*

*In this paper, we integrate crown features derived from images with stereo matching, and develop a model-based approach for reconstructing conifer-crown surfaces. The model is based on the fact that most conifer crowns are a form of solid geometry. We model a conifer crown as a generalized hemi-ellipsoid, establish the optimal tree model using a geometric equation, and apply the optimal tree model to guide a conventional pyramidal image matching in crown-surface reconstruction. The effectiveness of the approach is illustrated using an example of a redwood tree on 1:2,400-scale aerial photographs.*

## Introduction

A description of three-dimensional (3D) crown shape is useful in estimating the amount of foliage and the photosynthetic activity of trees. In forest inventory, parameters about crowns sometimes are collected such as diameter, height, closure, etc. Crown width (i.e., crown diameter) and height are important inputs to forest models (Deutschman et al., 1997), and are critical in modeling forest fires (Keane et al., 1999).

It is a time-consuming and labor-intensive process to measure crown diameter and height in the field, let alone measure the 3D crown surface. This led us to develop photo-ecometrics techniques for forest inventory (Gong et al., 1999). Aerial photography provides a practical means for tree measurement. Large-scale aerial photographs have long been used for measuring such parameters. Andrews (1936) derived tree height from aerial images in a stereo pair as early as in the 1930s. Tree height readings from 1:1,000-scale aerial photographs using a stereoplotter were found even more accurate than field measurements using tapes and clinometers (Kovats, 1997). Moessner (1949) developed a crown-density scale as a reference to interpret crown closure. Sayn-Wittgenstein (1961) applied crown characteristics (e.g., crown density, size, and marginal and apex shape) to tree species recognition. Crown information

is estimated most easily from aerial photos. However, the approaches are mainly based on visual interpretation. As a consequence, the process is less efficient, is subjective, and is error-prone (Biging et al., 1991).

Precise measurement of crowns from aerial photographs requires relatively accurate crown surface data. Due to the perspective view of aerial photographs, crown closure is overestimated when a stand is located far away from the principal points of the photographs. Theoretically, the parameters derived from orthophotos are free from the displacement influences. 3D crown surface data are needed to generate orthophotos from perspective photos.

Another requirement for crown-surface data comes from automated photointerpretation for forestry applications. As both the computing power and spatial resolution of remotely sensed data improves, more attention is being paid to individual tree-based photointerpretation (Gougeon, 1993; Gougeon, 1995; Pollock, 1996; Larsen, 1998). Although high-resolution photos capture information on individual trees, the displacement of a crown surface is large when measured in pixels. Current work in this field has focused on tree delineation using spectral information from monocular images. When forest photointerpretation results are input into a geographic information system (GIS), the coordinate data contain errors due to the perspective view of aerial photography. To eliminate the geometric errors, we need to use the 3D crown coordinates to orthorectify the aerial photographs.

Obviously, the marriage of crown-surface and spectral information will substantially benefit tree delineation, and crown-surface data can be used to produce orthographic tree maps for input into a GIS. Literature on crown-surface reconstruction is rather limited. Laser range detection (LIDAR: LIght Detecting And Ranging), radar interferometry, and photogrammetry are three major techniques for surface reconstruction. Airborne laser scanning systems detect range using laser pulses in the visible or near infrared wavelengths. To measure crown-surface heights, a LIDAR records multiple echoes; the first one is supposed to be reflected from the outer surface of a crown while the last from the ground after penetrating through the canopy. Crown-surface heights can be derived by subtracting the first range reading from the last. The penetration ability of a laser pulse is critical to the quality of surface reconstruction. It was found that, with near vertical incident angles of laser systems, 20 to 40 percent penetration rates were ex-

Center for Assessment and Monitoring of Forest and Environmental Resources, and Department of Environmental Science, Policy, and Management, 151 Hilgard Hall, University of California, Berkeley, CA 94720-3110 (gong@nature.berkeley.edu).

P. Gong is also with International Institute for Earth System Science, Nanjing University, Nanjing 210093, China.

pected through coniferous and deciduous forests. In particular, the penetration capability of laser through dense forests remains questionable (Ackermann, 1999). The requirements of high sampling rate, high signal-to-noise ratio, and multiple-echo recording capability for crown-surface measurement would make such a system quite expensive.

Radar interferometry detects elevation by phase correlation of radar echoes received by two radar antennas or by the same antenna at two fixed locations. Height can be acquired at an accuracy of centimeters. Space-borne interferometric radar (around 30 m resolution) has been used in earthquake monitoring, glacier movement monitoring, and digital elevation model (DEM) generation. The only research found on tree-crown characterization was the use of 1.5-m resolution airborne interferometric synthetic aperture radar (SAR) data at X- and C-bands over tropical rain forests in Indonesia (Hoekman and Varekamp, 1998; Varekamp and Hoekman, 1998). The results show that the interferometrically derived tree heights are underestimated.

Stereoscopic surface reconstruction from digital images is an important field of computer vision and photogrammetry. Both computer vision and photogrammetry use image matching methods to reconstruct surfaces. Photogrammetry is commonly used as the standard approach to terrain surface generation. However, photogrammetric efforts to generate crown surfaces are rare. Instead, trees are usually treated as undesired "disturbance" to be eliminated in photogrammetric operations. Gong et al. (2000) tested the use of digital photogrammetry for oak woodland monitoring. They suggested that digital surface models (DSM) that contain the elevation of landscape features such as buildings and tree canopies, rather than the commonly used digital elevation models (DEM) that only describe terrain heights, be used for land-change monitoring.

It is a challenge to reconstruct crown surfaces using photogrammetry, particularly for conifers. In a recent test made by Quackenbush et al. (1999), a Desktop Mapping System (DMS®) was used to derive tree canopy surfaces from aerial photographs scanned at a 1-m spatial resolution. They concluded that canopy-surface reconstruction was unsuccessful due to the constraint of the package used. Our experiments with a number of other commercial softcopy photogrammetry packages lead to the same conclusion. Current commercial packages are not designed to adequately extract tree-crown surfaces. There is a lack of algorithms for 3D information extraction for tree crowns.

We also conducted experiments to measure tree height through visual stereo matching using the digital photogrammetric programs in PCI® and VirtuoZo®. We found that it was possible to determine tree heights precisely as long as the corresponding treetops on the left and right images could be visually identified on the computer screen (Gong et al., 2000). Those experiments prove that stereoscopic images contain sufficient information for height measurements. This led us to further explore automated crown reconstruction algorithms. We aim to solve one of the most difficult problems in digital photogrammetry, that is, to reconstruct conifer-crown surfaces.

## Methods

We took the photogrammetric approach to reconstructing crown surfaces for the following reasons: first, aerial photography is one of the most widely used remote sensing tools in forestry. A large number of air photos are available; second, we are able to acquire both spectral imagery and surface spatial information with aerial photography.

### A Model-Based Strategy for Image Matching

The algorithm for image matching or correspondence point finding in a stereo pair is the core of photogrammetric surface reconstruction. Current image matching algorithms in photogrammetry are a sort of "blind matching." They do not use any prior knowledge during the matching process. The failure of photogrammetric methods in crown-surface reconstruction is that, when the algorithms match over a tree crown, they are not aware of the existence of a crown surface, and they do not treat the matching process with special care. The focus of this paper is on how to advise the matching algorithms with crown information. We propose a model-based image matching approach to solving this problem by introducing a tree model to guide the matching process.

Maitre and Luo (1992) applied geometric models to improve stereo reconstruction of buildings. They first utilized a regular stereo matching algorithm to get an initial disparity map of buildings, and then segmented the images into features. For each feature, they modeled the disparity as either a planar or a quadratic shape. Their approach demonstrates the algorithm's potential in reconstructing urban scenes. To apply their idea to crown-surface reconstruction, however, we anticipate the following potential problems. The first is segmentation. In a forest scene, to delineate individual crowns from their background is a difficult task (Gougeon, 1995). The second problem is the initial disparity because the sharp surface of coniferous crowns causes problems in conventional stereo matching, and the initial disparity map derived from regular matching algorithms is not sufficiently reliable to subsequently serve the modeling purpose.

Our model-based approach to crown-surface reconstruction relies on three components: geometric tree model construction, disparity prediction from tree models, and integration of the model predictions into image matching. Tree models are developed from the original images. We propose the following model-based strategy to reconstruct crown surfaces:

1. With an estimate of the ground disparity range, generate a smooth ground surface using conventional stereoscopic technique, and fill the gaps using interpolation. Trees are usually the gaps.
2. Identify the top of each individual tree on the left and right images, and calculate its coordinates in the ground coordinate system.
3. Estimate tree height by subtracting the corresponding ground elevation from the elevation of the treetop.
4. Based on the tree height and other parameters such as the maximum and minimum crown size, determine the optimal tree model of the tree.
5. Apply the optimal tree model to predict an initial crown disparity.
6. Integrate the predicted crown disparity into pyramidal stereo matching by using it as the initial disparity for the final level matching.
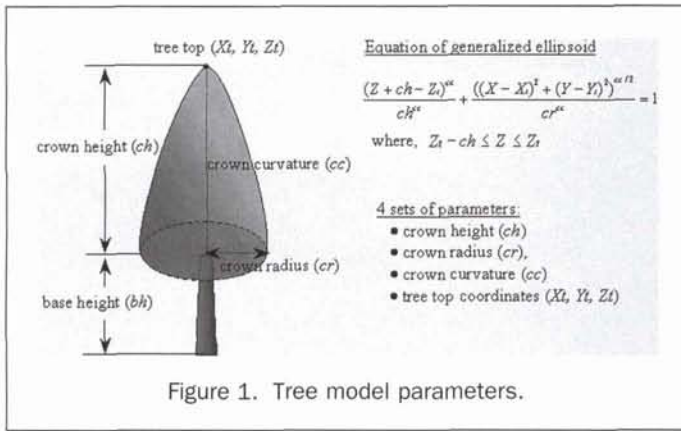
### Tree Models

The form of tree crowns is related to environment. In northern and alpine environments, conifers are adapted to grow in a conical shape, due to strong selection pressures of snow, ice, and wind (Barnes et al., 1998).

Biging and Gill (1997) gave a comprehensive summary of crown modeling, and applied stochastic ARMA (Auto-Regressive Moving Average) models in conifer-crown profile modeling using time series analysis. Though crown margins are stochastic in nature, we adopted geometric models for their simplicity in parameterization. Horn (1971) proposed the following equation as a general model for the 2D vertical profile of a crown envelope:

$$\frac{z^{cc}}{ch^{cc}} + \frac{y^{cc}}{cr^{cc}} = 1$$

where $ch$ and $cr$ are the vertical and horizontal dimensions of a

Figure 1. Tree model parameters.

Equation of generalized ellipsoid

$$\frac{(Z + ch - Z_t)^{\alpha}}{ch^{\alpha}} + \frac{((X - X_t)^2 + (Y - Y_t)^2)^{\frac{1}{2}\alpha n}}{cr^{\alpha}} = 1$$

where, $Z_t - ch \leq Z \leq Z_t$

4 sets of parameters:
- crown height $(ch)$
- crown radius $(cr)$,
- crown curvature $(cc)$
- tree top coordinates $(X_t, Y_t, Z_t)$



(a) $ch=20m, cr=3m, cc=0.8$

(b) $ch=20m, cr=3m, cc=1.0$

(c) $ch=20m, cr=3m, cc=1.5$

(d) $ch=10m, cr=7m, cc=2.0$

Figure 2. Examples of the tree model.

crown, respectively, and $cc$ is a positive adjusting coefficient for crown curvature. When $cc = 1$, the curve is a straight line, and $cc < 1$ indicates an increasingly upwards concave curve, while $cc > 1$ represents an increasingly downwards concave curve. To generate templates for the tree delineation purpose on monocular MEIS (Multi-detector Electro-optical Imaging Scanner) images, Pollock (1996) extended Horn's formula into 3D, and modeled a crown envelope with a generalized ellipsoid: i.e.,

$$\frac{z^{cc}}{ch^{cc}} + \frac{(x^2 + y^2)^{cc/2}}{cr^{cc}} = 1$$

where $(x, y, z)$ are the coordinates on the crown surface. We adopted Pollock's crown model for geometric crown modeling. For our purpose of applying the crown model to guide stereoscopic image matching, we need to know the location of a crown. Our tree model is described by four parameters as illustrated in Figure 1: ground coordinates of the treetop $(Xt, Yt, Zt)$, crown height $(ch)$, crown radius $(cr)$, and an adjusting coefficient for crown curvature $(cc)$. Once these parameters are known, the ground coordinates $(X, Y, Z)$ of any point on the crown surface can be modeled by

$$\frac{(Z + ch - Z_t)^{cc}}{ch^{cc}} + \frac{((X - X_t)^2 + (Y - Y_t)^2)^{cc/2}}{cr^{cc}} = 1$$

where $Z - ch \leq Z \leq Z_t$.

Figure 2 shows the geometric shapes of crowns with various dimensional parameters. The first three (Figures 2a, 2b, and 2c) are a 20-m-high, 6-m-wide conifer-crown with a curvature of 0.8, 1.0, 1.5, respectively. The last one (Figure 2d) mimics a rounded hardwood crown 10 m high and 14 m wide. Although this model over-simplifies crowns in the real world, it may be adequate to serve as an initial condition for guiding the crown-surface reconstruction process. Our objective is to reconstruct the true crown-surface coordinates through the guidance of such a model so that more precise measurements of the crown surface can be made.

We determine the optimal tree model interactively in this paper, but the process can potentially be automated as was done by Larsen and Rudemo (1998) and Pollock (1996). The first step is to identify the top of a tree on images. The top of a conifer usually is not quite recognizable when it is viewed vertically; however, off-nadir views are more informative. In addition, to ensure each point on a conifer crown may be viewed from two different directions for the purpose of disparity derivation, a stereo triplet was used in this paper (Figure 3).

A triplet forms three stereo pairs: the left-right pair, the left-middle pair, and the middle-right pair. The ground coordinates
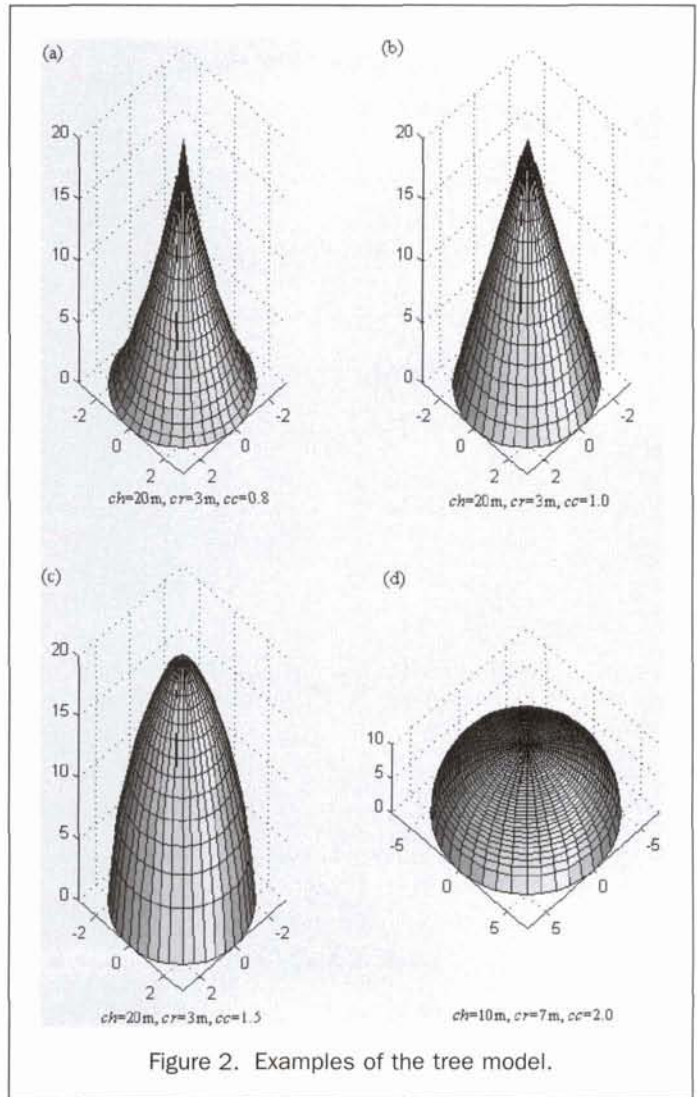
of a treetop can usually be derived from the left-right pair. The elevation of a tree base can be roughly estimated from a stereo pair. Dimensional parameters about the crown can also be determined interactively from the images.

### Image Matching Scheme

From a historical point of view, correspondence algorithms for stereopsis can be divided into two groups: the correlation-based (or area-based) methods and the feature-based methods (Sonka et al., 1999). In feature-based matching, features such as corners and, more often, edges have to be automatically identified in the images before matching takes place. However, features in a natural forest scene are hard to define, and are often unidentifiable in the images. We used the area-based image-matching scheme. Area-based correspondence algorithms are based on the assumption that pixels in correspondence have similar intensities. The intensity of an individual pixel does not give sufficient information. Thus, intensities of several neighboring pixels are considered.

The correspondence problem is inherently ambiguous due to factors such as noise, varying viewing direction, and perspective distortion. Thus, the intensities of the corresponding pixels will differ in the two images. For a particular point in one image, there are usually several matching candidates in the other image, and the true candidate does not necessarily produce the maximum similarity. Correspondence ambiguities can
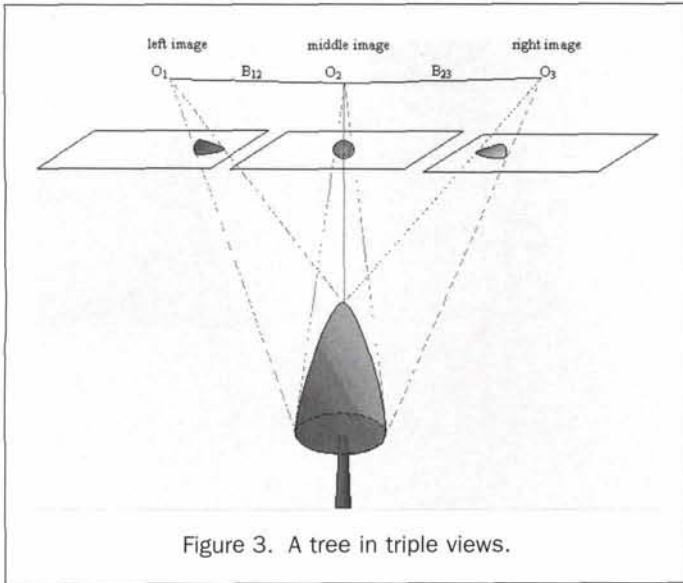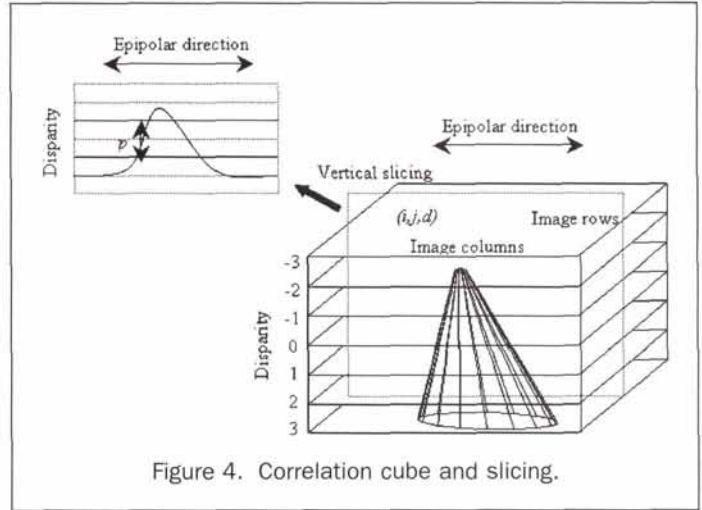
Figure 3. A tree in triple views.



Figure 4. Correlation cube and slicing.

be reduced with additional constraints. In Marr's original image matching theory (Marr, 1982), the following three constraints were introduced:

- Photometric compatibility constraint: Pixels in correspondence have similar intensities;
- Uniqueness constraint: A pixel in one image can correspond to only one pixel in the other image; and
- Disparity continuity constraint: Disparity varies smoothly almost everywhere over the image.

Other important constraints developed by others include

- Epipolar constraint: The matching points must lie on the corresponding epipolar lines of the two images. This constraint reduces the two-dimensional search space into a one-dimensional search space.
- Disparity limit constraint: This constraint limits the disparity search within a certain range.

We adopt the image-matching algorithm by Sun (1997) as the basic matching scheme because it can make use of all the above constraints. Similarity (or dis-similarity) is the guiding principle for solving the correspondence problem. Similarity measures have been diversified, and their performance and computation costs vary. Among them, the cross-correlation coefficient has been used most widely due to its independence of variations in brightness and contrast.

The result of the correlation calculation forms a cube containing the correlation coefficients (Figure 4). The epipolar constraint and the disparity limit constraint are used in the generation of the correlation cube. Let the range of disparity limit be $[-D, D]$, and the input left and right epipolar images be of size $row*col$; then, the correlation cube is generated by calculating the correlation coefficients between the left image and the right image shifted from $-D$ to $D$ along the epipolar direction. The column of the cube is along the epipolar direction, and the vertical dimension is disparity. The value at pixel $(i, j, d)$ is the correlation coefficient of pixel $(i, j)$ on the left image when disparity is $d$ $(-D \leq d \leq D)$ The size of the cube depends upon the image size $(row*col)$ and the disparity range $(2*D + 1)$.

One advantage of such a correlation cube is that it allows us to combine multiple constraints in determining the disparity map by searching the cube. The simplest and often used algorithm is to find the maximum correlation under a threshold constraint. However, the disparity continuity constraint is ignored. We treat the task as finding a smooth surface in the cube that maximizes its total correlation and simultaneously uses

the following constraints: photometric compatibility, uniqueness, and disparity continuity.

We simplify the 3D surface searching problem to a 2D path optimization problem by slicing the correlation cube along the epipolar direction. In a slicing plane, the horizontal dimension is along the epipolar direction, while the vertical dimension is the range of disparity. For each slicing plane, we search for the optimal path from the left to the right through the correlation matrix using dynamic programming techniques to maximize the total correlation on the path. The position of the path indicates the best disparity for this slice.

Dynamic programming techniques have advantages in solving the optimization problem. Image matching by dynamic programming is a global matching approach, which seeks for the optimal solution globally instead of locally. The length of a path here is defined as the summation of the correlation coefficients along the path. The best path holds the longest length when the disparity continuity constraint is satisfied. To define the smoothness of a path, a $p$th-order path is introduced. A $p$th-order path searches the next cell up and down in the range of $[-p, p]$ from the current cell (Buckley and Yang, 1997). In this sense, parameter $p$ serves as a smoothness constraint.

The effectiveness of a coarse-to-fine pyramidal matching strategy is widely recognized. An image pyramid consists of a hierarchy of multi-resolution images, with the lower levels containing finer resolution data than the upper levels. The resolution from one level to the next is typically increased by a scale factor of 2 or 3. The number of levels is determined by the disparity range and the scale factor of the pyramid. Pyramidal image matching is implemented in a coarse-to-fine manner. The matching starts at the highest level first, where the image is small. The disparity outputs at this level are then used as initial values to restrict the disparity search at the next finer level. This continues to the finest resolution level. This strategy not only significantly reduces the computation because only a small range needs to be searched on a small image at each level, but also increases the reliability of image matching by matching both globally for overviews at upper levels and locally for details at lower levels.

We use $scale = 3$ as the scale factor of the pyramid in our algorithm because this is more computationally economic. The average of a 3 by 3 neighborhood makes a pixel at a higher level. In addition to its computational efficiency and reliability, the pyramidal structure has additional advantages in our model-based matching scheme: (1) it makes the correlation cube as small as $(2*scale + 1)*row*col$ at each level; (2) it can focus on different levels of details; and, more importantly, (3)
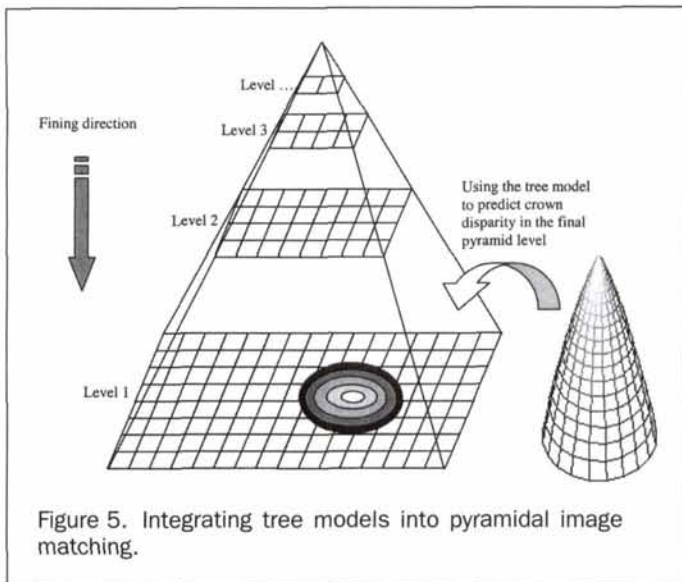
Figure 5. Integrating tree models into pyramidal image matching.



Figure 6. Epipolar images in the three stereo pairs formed with triple images.

it allows us to add geometric models at any level. This is desirable in integrating tree models into the above conventional image-matching scheme.

### Incorporating the Tree Model in Image Matching

Our goal is to let the matching algorithm know the characteristics of a crown surface during image matching. In a conventional matching scheme, very little prior knowledge about the objects is needed. In crown-surface reconstruction, however, we have a rough idea of crown shape through establishment of the optimal tree model. Conifer-crowns in natural forests usually have solid geometric shapes, a conical shape for young trees and a parabolic shape for mature trees. We integrate a geometric tree model into image matching by using the model as a new constraint, the geometric shape constraint. Once we know the tree model from image analysis, we can calculate the ground coordinates of each point on the crown, and then we can predict crown disparities in any image. The predicted disparity map serves as a guide to find correspondence. The correspondence search can be limited to a small range, usually a couple of pixels, around the predicted disparities. Therefore, we can introduce the tree model only at the final level of the pyramidal matching scheme for a minor adjustment. Because trees are specially treated at the final level, the other levels of pyramidal matching can concentrate on matching for ground objects, by setting the disparity limit range specifically for the ground. The ground is relatively smooth, and can usually be well handled by conventional image matching approaches. The output disparities at the second level from the last are modified by the predicted disparities from tree models before they are used as the initial disparity map at the final stage (Figure 5). That is, the initial disparity map at the final level is composed of two different sources: (1) the disparities obtained with a conventional image matching algorithm at the previous level, and (2) the crown disparities predicted from tree models.

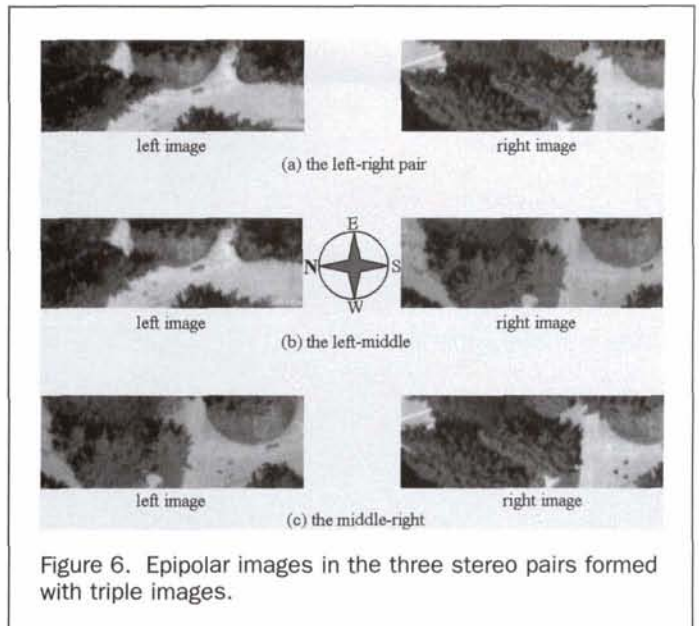When the dynamic programming algorithm searches for disparity paths in the correlation cube at the final level, the order of the paths, $p$, can be set to various values from 0 to *scale*, depending on the confidence in the optimal tree model. If the tree model perfectly describes the crown surface, then set the order $p$ to zero, which means no adjustment is needed. If the tree model is only a rough approximation of the real crown surface, then $p$ needs to be increased, and this will introduce more variations into the reconstructed crown surface.

## Experimental Results

We performed the test with a redwood tree at the campus of University of California at Berkeley (122.38°W, 37.62°N) using 1:2,400-scale color aerial photographs. The photos were taken around 1410 hours on 23 May 1994 under clear sky conditions with an aerial camera having a focal length of 152.888 mm. The sunlight illuminated the ground from the southwest (AZ = 234.44°) at an elevation angle of 71.80°. This redwood tree was visible on three overlapping photos. These photos were scanned and digitized at 250 DPI, making the pixel resolution approximately 24 cm on the ground. The photographic station locations and camera attitudes were solved for through orientation procedures (Table 1). The three photos form three stereo pairs. The green-band epipolar images covering the tree of interest are shown in Figure 6. More parts of the tree-crown are visible on the middle-right pair (Figure 6c), so we focused on this pair. The periodical patterns in the images caused by layered stretching branches make the matching task more difficult.

Both conventional image matching and the model-based approach were implemented and applied for a comparison. We first generated the crown surface of this tree using the conventional image-matching algorithm described in the image matching section. With the tree-crown disparities considered, the disparity range is estimated as $[-30, 24]$ for the middle-right pair. For pyramid matching efficiency, we use $[-27, 27]$ after a centralization as the disparity limit in the surface reconstruction. The resulting disparity map is shown in Figure 7a.

TABLE 1. PHOTOGRAPHIC ORIENTATION ELEMENTS

| Photo Name | Flight Station Coordinates (X, Y, Z) in Meters | Camera Attitude ($\varphi$, $\omega$, $\kappa$) in radians |
|---|---|---|
| The Left Image | (4172.145, 3999.740, 399.095) | (0.00792, 0.00259, 0.00023) |
| The Middle Image | (4370.708, 4002.312, 402.907) | (0.01269, −0.00455, −0.00404) |
| The Right Image | (4576.447, 4003.478, 404.708) | (−0.00663, −0.00543, −0.00316) |

Figure 7. Results from the regular image matching approach. (a) Disparity map. (b) Surface model.



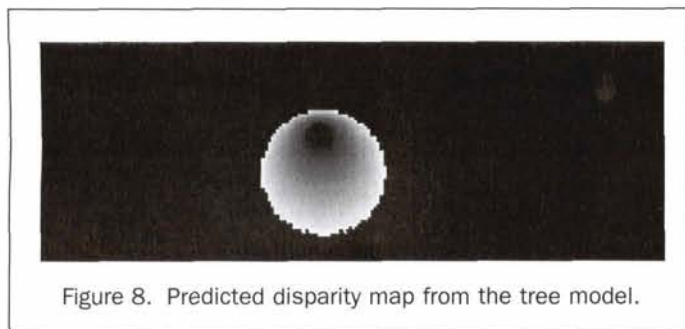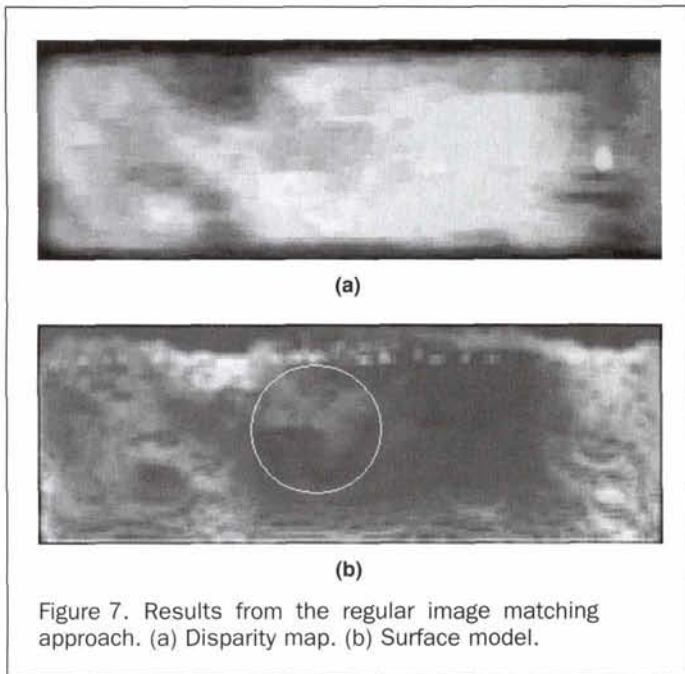Figure 8. Predicted disparity map from the tree model.

Figure 7b is the reconstructed digital surface model. The red-wood tree of interest (circled by the white line in Figure 7b) is flattened so seriously that the tree turns out to be only 7 meters high. Though having taken many constraints into consideration, the conventional matching scheme does not work well. It is necessary to introduce the model-based approach.

In the model-based approach, we need to determine the optimal tree model for this tree. The 3D ground coordinates of the treetop were acquired from the left-right pair (Figure 6a). The treetop coordinates are (col: 88, row: 28) in the left image, and (col: 68, row: 28) in the right image. Its ground coordinates were thus calculated as 4366.60 m, 4056.94 m, and 49.47 m). The elevation of the tree base was determined to be 25.15 m. Therefore, the tree height was roughly estimated as 24.32 m. The dimension of the crown was determined interactively. The parameters of this tree model turned out to be: $(X_t, Y_t, Z_t)$ = (4366.60 m, 4056.94 m, 49.47 m), $ch$ = 21.8 m, $cr$ = 4.8 m, $cc$ = 1.1, $bh$ = 2.5 m.

Figure 8 shows the crown disparity map predicted from the tree model. Because special care has been paid to the crown, we can focus on the ground in the upper-level pyramidal image matching. We narrow the disparity limit range down to [24, 30] for the ground surface in this example. The algorithm mainly matches for the ground surface at the high levels of the pyramid. At the final level, we modify the output disparity map from the higher level with the predicted crown map, and use it as the initial disparity map in the final matching.

The path order $p$ can be specified between 0 and 3. When specifying path order $p = 1$, the algorithm has a ±1-pixel flexibility in controlling path smoothness, corresponding to about 0.4 m in the ground coordinate system. A larger $p$ gives the crown matching more freedom in the disparity search, and therefore allows for more variations in the reconstructed crown surface. When the crown is not well defined by the optimal tree model, a larger $p$ may give more realistic results.

The results using $p = 1$ are shown in Figure 9. Figures 9a and 9b are the derived disparity map and the reconstructed surface map, respectively. Because the east side of the crown is occluded in both images, gaps are found in this area in the surface map. After filling the gaps using interpolation techniques, the final surface map is shown in Figure 9c. Corresponding maps obtained using $p = 2$ are shown in Figure 10. Comparing Figure 10 with Figure 9, we can see that there is no significant difference between the two surface maps, though the one derived using $p = 2$ has slightly more elevation variations. On both maps, the tree of interest turns out to be 25.14 m high. This indicates that this tree has a regular crown shape and that the tree model well describes this tree. We use the surface of $p = 2$ in the following analysis.

A field measurement was conducted on 24 October 1999. Because it is very difficult to directly measure a crown surface on the ground, tree height, base height, and crown radii from eight directions were measured using clinometers and tapes. Ground observations and corresponding plots from the reconstructed crown surface are illustrated for a comparison in the upper row and the lower row of Figure 11. Ground pictures of the tree were taken from the west and the south (Figures 11a and 11b), respectively. The measured crown radii are plotted in Figure 11c. The ground observations indicate that this tree is conical in shape. The profiles of the reconstructed crown surface are shown in Figure 11d (west view), Figure 11e (south view), and Figure 11f (crown contours at a 2 m interval). Comparing these profiles with the corresponding ground observations, we can see that they are mostly consistent. The stretching branch marked at **A** in the photo from a west view (Figure 11a) is also visible in the profile (marker **A** in Figure 11d). The marked points **B** and **C** in the profile from a south view (Figure 11e), however, do not have matching features in the corresponding ground photo (Figure 11b) because they are the results of gap filling in the digital surface model. They are on the east side of the crown, and invisible under this imaging configuration.
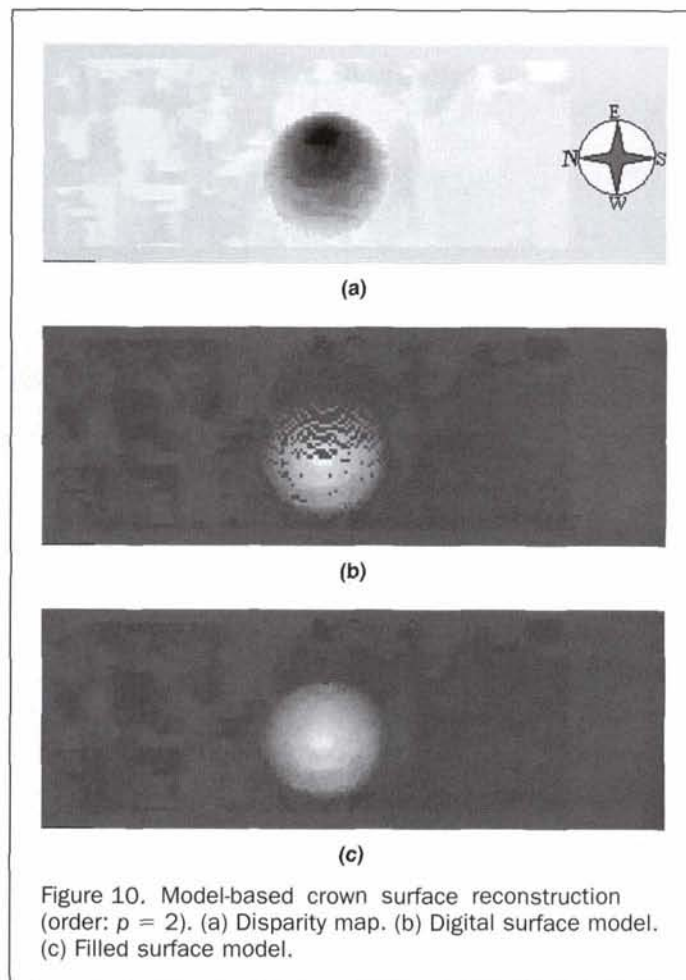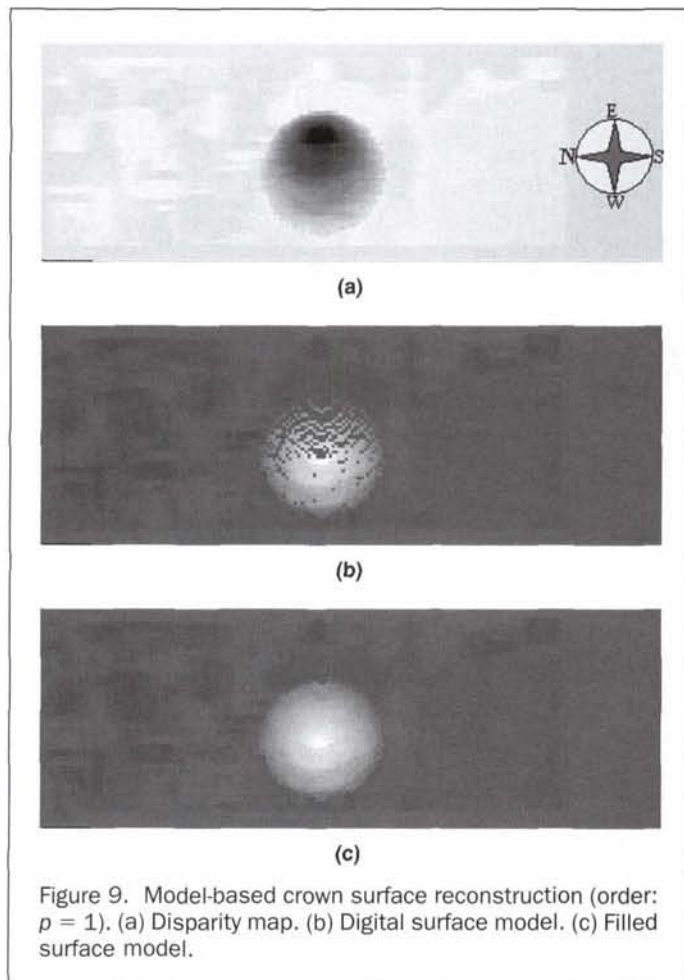
The reconstructed height of this redwood tree is 25.1 meters, while it was measured as 27.4 meters in the field, which is underestimated by 2.3 meters. These photos were taken (in 1994) five years earlier than the field measurements (in 1999). It is possible for a redwood tree to grow by this amount during this period. This underestimation may also be partially caused by the fact that the very sharp tip of a conifer may not be captured during the photo imaging and scanning stages.

We draped the original middle image on the top of the reconstructed surface to view the surface in 3D. The northeast, southeast, northwest, and southwest views are shown in Figures 12a, 12b, 12c, and 12d, respectively. The redwood tree looks realistic from all these directions.

## Discussions

From the above experiment, we can see that the crown-surface reconstruction can be considerably improved after a tree model is introduced into a conventional image matching algorithm. Although we have demonstrated the potential of such a model-based approach to crown-surface reconstruction, many problems still exist.

An optimal tree model may not precisely describe a tree surface, especially when the tree is in an irregular shape. Con-

Figure 9. Model-based crown surface reconstruction (order: $p = 1$). (a) Disparity map. (b) Digital surface model. (c) Filled surface model.



Figure 10. Model-based crown surface reconstruction (order: $p = 2$). (a) Disparity map. (b) Digital surface model. (c) Filled surface model.

sequently, the model-based approach may not produce an adequate surface even with a large path order. The approach discussed in this paper can be implemented as an iterative procedure. When our knowledge about tree height and canopy shape is poor, we can begin with a rough tree surface model with approximate tree parameters for the model-based approach. The output from the first round of model-based matching can be used as an initial condition in the next round of model-based matching for gradual adjustment. This procedure can be repeated until the improvement converges.

It is difficult to obtain an optimal tree model. We dealt only with a single tree in our example, and determined the optimal tree model interactively. Our work is ongoing to facilitate the tree model acquisition process so as to meet the requirement for tree-crown surface reconstruction for an entire stereo image coverage. Relevant research has been done on monocular images. Pollock (1996) developed optimal tree models using crown template matching for tree delineation, and Larsen and Rudemo (1998) detected conifer treetops using a similar technique. We need to determine the ground coordinates for treetops in our tree model. We will use multi-ocular images for optimal tree model development. The multi-ocular approach is expected to produce better tree models than do the monocular approaches.

This paper uses a single tree as an example, but the proposed approach is readily applicable to sparse tree stands. The problem becomes complicated for dense forest stands where trees occlude each other. Occlusion will be treated in future research. A user-friendly interface is desirable for model-based crown analysis because human-machine interaction becomes necessary for complicated forest stands such as dense or uneven-aged stands.

## Conclusions

Tree-crown surface reconstruction is a difficult problem. It is not surprising that the current photogrammetric algorithms are not successful because crown surfaces are sharp and irregular. Although most of the commercially available image-matching algorithms have many factors as control and constraints, they still fail to adequately reconstruct tree-crown surfaces. Introducing tree-crown models into surface reconstruction dramatically improves this situation. The generalized ellipsoidal tree model can well describe most conifers. Our results indicate that crown-surface reconstruction through integration of tree-crown models with conventional pyramidal image matching is a good strategy. In the pyramidal image matching algorithm, slowly varying ground surface coordinates are extracted at the higher levels. At the final level, tree models are integrated to guide image matching for local adjustment of disparities. The degree of adjustment can be controlled by a parameter, the order $p$ of the optimal path in dynamic programming techniques. This ensures that the image-matching algorithm will find the correct correspondence on a tree-crown in a proper range. When a tree is irregular in shape, or an optimal tree model is not adequate, a larger $p$ value may help by giving more freedom in the image matching process. In addition, a model-based iterative image-matching algorithm may be implemented to achieve better results for conifer-crown surface reconstruction.
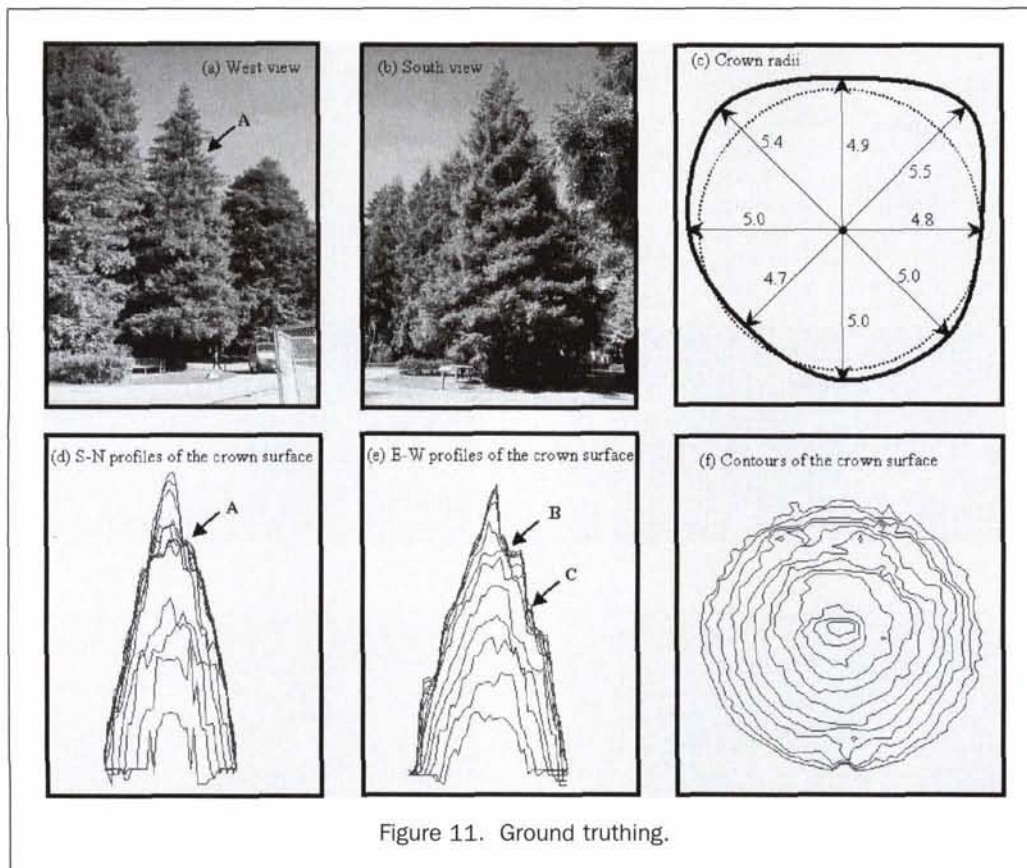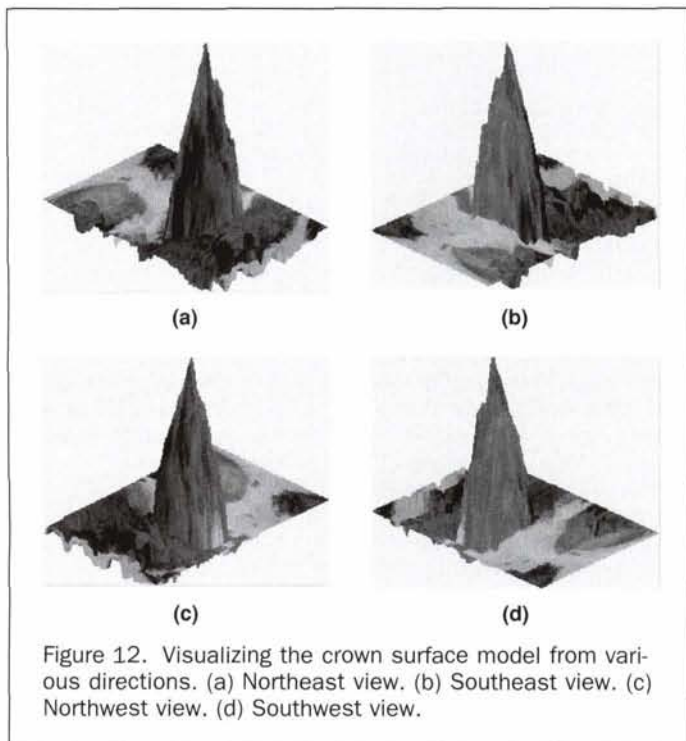
Figure 11. Ground truthing.



Figure 12. Visualizing the crown surface model from various directions. (a) Northeast view. (b) Southeast view. (c) Northwest view. (d) Southwest view.

The proposed model-based image-matching algorithm has demonstrated its effectiveness in conifer-crown surface reconstruction. The model-guided image matching approach has potential in solving other surface reconstruction problems when prior knowledge regarding the shapes of objects is available.

## References

Ackermann, F., 1999. Airborne laser scanning—Present status and future expectations, *ISPRS Journal of Photogrammetry and Remote Sensing*, 54(2–3):64–67.

Andrews, G.S., 1936. Tree heights from air photographs by simple parallax measurements, *Forestry Chronicle*, pp. 1–54.

Barnes, B.V., D.R. Zak, S.R. Denton, and S.H. Spurr, 1998. *Forest Ecology, Fourth Edition*, John Wiley & Sons, New York, N.Y., 774 p.

Biging, G.S., R.G. Congalton, and E.C. Murphy, 1991. A comparison of photointerpretation and ground measurements of forest structure, *Proceedings of the 57th Annual Meeting of ASPRS*, 23–29 March, Baltimore, Maryland, pp. 6–15.

Biging, G.S., and S.J. Gill, 1997. Stochastic models for conifer tree crown profiles, *Forest Science*, 43(1):25–34.

Buckley, M., and J. Yang, 1997. Regularised shortest-path extraction, *Pattern Recognition Letters*, 18(7):621–629.

Deutschman, D.M., A.L. Simon, C. Devine, and L.A. Buttel, 1997. Scaling from trees to forest: Analysis of a complex simulation model, *Science*, 277(5332): www.sciencemag.org/feature/data/deutschman/index.htm.

Gong, P., G.S. Biging, S.M. Lee, X. Mei, Y. Sheng, R. Pu, B. Xu, K.P. Schwarz, and M. Mostafa, 1999. Photo-ecometrics for forest inventory, *Geographic Information Sciences*, 5(1):9–14.

Gong, P., G.S. Biging, and R. Standiford, 2000. The potential of digital

surface model for hardwood rangeland monitoring, *Journal of Range Management*, 53:622–626.

Gougeon, F.A., 1993. Individual tree identification from high resolution MEIS images, *Proceedings of the International Forum on Airborne Multispectral Scanning for Forestry and Mapping*, 13–16 April 1992, Val-Morin, Quebec, Canada, pp. 117–128.

———, 1995. A crown-following approach to the automatic delineation of individual tree crowns in high spatial resolution aerial images, *Canadian Journal of Remote Sensing*, 21(3):274–284.

Hoekman, D.H., and C. Varekamp, 1998. High-resolution single-pass interferometric radar observation of tropical rain forests trees, *Proceedings of the Second International Workshop on Retrieval of Bio & Geo-Physical Parameters from SAR Data for Land Applications*, 21–23 October, Noordwijk, The Netherlands, European Space Agency (ESA) SP 441, pp. 233–240.

Horn, H.S., 1971. *The Adaptive Geometry of Trees*, Princeton University Press, Princeton, New Jersey, 144 p.

Keane, R.E., S.A. Mincemoyer, K.M. Schmidt, J.P. Menakis, and J.L. Garner, 1999. Fuels and vegetation mapping for fire management on the Gila National Forest, New Mexico, *Proceedings, 1999 Annual Conference of the American Society for Photogrammetry and Remote Sensing*, 17–21 May, Portland, Oregon (CD-ROM).

Kovats, M., 1997. A large-scale aerial photographic technique for measuring tree heights on long-term forest installations, *Photogrammetric Engineering & Remote Sensing*, 63(6):741–747.

Larsen, M., and M. Rudemo, 1998. Optimizing templates for finding trees in aerial photographs, *Pattern Recognition Letters*, 19(12):1153–1162.

Maitre, H., and W. Luo, 1992. Using models to improve stereo reconstruction, *IEEE Transactions on Pattern Analysis and Machine Intelligence*, 14(2):269–277.

Marr, D., 1982. *Vision: A Computational Investigation into the Human Representation and Processing of Visual Information*, W. H. Freeman and Company, New York, N.Y., 397 p.

Moessner, K.E., 1949. A crown density scale for photo interpreters, *Journal of Forestry*, 47(7):569.

Pollock, R.J., 1996. *The Automatic Recognition of Individual Trees in Aerial Images of Forests Based on a Synthetic Tree Crown Image Model*, Ph.D Thesis, University of British Columbia, Vancouver, Canada, 172 p.

Quackenbush, L.J., P.F. Hopkins, and G.J. Kinn, 1999. Developing derivative products from high resolution digital aerial imagery, *Proceedings, 1999 Annual Conference of the American Society for Photogrammetry and Remote Sensing*, 17–21 May, Portland, Oregon (CD-ROM).

Sayn-Wittgenstein, L., 1961. Recognition of tree species on air photo by crown characteristics, *Photogrammetric Engineering*, 27(5):792–809.

Sonka, M., B. Hlavac, and R. Boyle, 1999. *Image Processing, Analysis, and Machine Vision, Second Edition*, PWS Pub., Pacific Grove, California, 770 p.

Sun, C., 1997. A fast stereo matching method, *Proceedings, Digital Image Computing: Techniques and Applications*, 10–12 December, Auckland, New Zealand, pp. 95–100.

Varekamp, C., and D.H. Hoekman, 1998. An inversion algorithm for automated retrieval of tree crown characteristics from high-resolution interferometric SAR data, *Proceedings of the Second International Workshop on Retrieval of Bio & Geo-Physical Parameters from SAR Data for Land Applications*, 21–23 October, Noordwijk, The Netherlands, European Space Agency (ESA) SP 441, pp. 241–244.

# Forthcoming Articles